Molecular Crystals and Liquid Crystals

ISSN: 1542-1406 (Print) 1563-5287 (Online) Journal homepage: http://www.tandfonline.com/loi/gmcl20

Investigation of structural and physical properties of $xSrO-(100-x)P_2O_5$ glasses

Zahra Ramzi, Samira Touhtouh, Wafaa Nachit, Khalil Benkhouja, M'hamed Taibi & Abdelowahed Hajjaji

To cite this article: Zahra Ramzi, Samira Touhtouh, Wafaa Nachit, Khalil Benkhouja, M'hamed Taibi & Abdelowahed Hajjaji (2016) Investigation of structural and physical properties of $xSrO-(100-x)P_2O_5$ glasses, Molecular Crystals and Liquid Crystals, 627:1, 97-105, DOI: 10.1080/15421406.2015.1137137

To link to this article: http://dx.doi.org/10.1080/15421406.2015.1137137

Published online: 13 May 2016.

MOL. CRYST. LIQ. CRYST.
2016, VOL. 627, 97–105
http://dx.doi.org/10.1080/15421406.2015.1137137

Taylor & Francis
Taylor & Francis Group

Investigation of structural and physical properties of $xSrO\text{-}(100\text{-}x)P_2O_5$ glasses

Zahra Ramzi[a,b], Samira Touhtouh[b], Wafaa Nachit[a,b], Khalil Benkhouja[a], M'hamed Taibi[c], and Abdelowahed Hajjaji[b]

[a]E2M_LCCA, Chemistry Department, Faculty of Sciences, UCD University,El Jadida, Morocco; [b]LabSIPE, ENSA, National School of Applied Sciences, UCD University,El Jadida, Morocco; [c]LPCMIO, Université Mohammed V-Agdal, Ecole Normale Supérieure Rabat

ABSTRACT

The structural and physical properties for $xSrO\text{-}(100\text{-}x)P_2O_5$ glasses, with $x = 30, 35, 40, 45$, and 50, were investigated. The amorphous state of samples was verified by X-ray diffraction (XRD). Substitution of P_2O_5 for SrO in the binary $SrO–P_2O_5$ glass decreases the molar volume and increase the density measurements from 1.98 to 4.01 g/cm^3. The Infra-Red (IR) and Raman spectra allow us to identify the network modifier role of Sr^{2+} ions and the structural network of these phosphate glasses which consists of branching (Q^3), middle phosphate tetrahedra (Q^2) and pyrophosphate (Q^1).

KEYWORDS

Phosphate glasses; Strontium; Network connectivity; Physical properties

1. Introduction

The interest in the investigation of vitreous oxide materials was stimulated by the many applications of these materials in the different fields of science and technique. Nowadays, the study of vitreous oxide materials represents a special field in the larger field of the material science.

Phosphate glasses, a special group of oxide materials, are interesting due to their properties such as: low glass transition temperatures, thermal expansion coefficients larger than those found for silicate glasses and glass formation takes place over a wide composition range [1, 2]. Many researchers have focused on phosphate glasses in the last years due to their diversified applications in technology, medicine, as biomaterials and in clinical dosimetry. Unfortunately, the chemical stability, such as hygroscopicity and volatility of phosphate glasses, generates a serious problem for any viable technological application. These hygroscopicity and volatility arise mainly because of the presence of phosphorous structural units with non-bridging oxygen atoms, which can react with moisture, forming. phosphoric acid, thus formed is detrimental to the glass and it volatilizes on heating. To improve the chemical stability of phosphate glasses a series of alkali, alkaline earth, rare earth and transition metal ions was added [3–6].

Strontium oxide does not form a glass alone incorporated in significant amounts into other glass-forming oxide systems such as vanadium, bismuth and phosphates. Sungkoog et al prepared glasses materials from the $xSrO\text{-}(100\text{-}x)\ V_2O_5$ ($x = 15$ to 45 mol%), The conduction

CONTACT Zahra Ramzi zahramzi80@gmail.com E2M_LCCA, Chemistry Department, Faculty of Sciences, UCD University, P.O. Box 20, 24000 El Jadida, Morocco

Color versions of one or more of the figures in the article can be found online at www.tandfonline.com/gmcl.

mechanism of these glasses was found to be a non-adiabatic electron conduction. The values for the activation energy of these glass systems varied significantly with increasing of SrO content [7]. Egorysheva et al, performed the physicochemical properties of glasses based on the SrO-Bi_20_3-B_20_3 systems, who found that the glass formation regions and studied the structural, the optical properties [8].

On Strontium phosphate-based glasses, several works have been carried out in the last decade, especially concerning an optimization of glass preparation, investigation of their properties and information about the glass structure. Shih et al, investigated the properties and the structure of UV-transmitting vitreous strontium zinc metaphosphate, who found that UV-transmitting phosphate glasses with transmittance greater than 70% at 250 nm were obtained using reagent-grade raw materials [9, 10]. But there are obvious shortcomings in the glass series: High thermal expansion coefficient and poor relative chemical durability. Luo et al investigated the thermal, chemical and optical properties of the strontium zinc borophosphosilicate $2Al_2O_3$-xSrO–(18-x) ZnO–$33.3P_2O_5$–$16.7B_2O_3$–$30SiO_2$ glass series, who found that the glass transition temperatures (Tg) and softening points (Td) vary within a small range. It was shown the chemical durability of the glasses increases when $x \leq 9$, and drops when $x \geq 9$. With the increasing SrO content, the UV transmittance of the glasses decreases mildly. The compositional dependence of E_{opt} shows a decrease trend with increasing SrO content [11]. Chu and al, studied optical and structural properties of SrO–Nb_2O_5–P_2O_5 glasses containing 0∼25 mol% Nb_2O_5 and 35∼60 mol% SrO, and found that Nb-phosphate glasses show refractive index increases monotonically with Nb_2O_5 content at the expense of transmittance, and specific coloring which occurs in ternary compositions with the ratio P_2O_5/SrO >1 [12].

Recently, Massera et al, investigated the effect of substituting SrO for CaO in silicate and phosphate bioactive glasses on the human gingival fibroblast activity, They noted that The addition of SrO in both silicate and phosphate glasses was assumed beneficial for proliferation and growth of human gingival fibroblasts due to Sr incorporation in the reaction layer at the glass surface and released in the cell culture medium [13].

The addition of SrO to phosphate glasses improves their chemical durability, thermal stability and other physical properties. The incorporation of strontium to the phosphate structural network is accompanied by depolymerization of the phosphate chains and the creation of non-bridging oxygens at the expense of bridging oxygens which can change the electrical, optical or magnetic properties of these glasses.

The aim of this study was the development of new binary strontium phosphate glasses for use as optical materials. xSrO-(100-x)P_2O_5 glass system is investigated by means of a few physical parameters, XRD, FT-IR spectroscopy, and Raman spectroscopy, in order to obtain detailed structural information about the glass network.

2. Experimental and methods

The xSrO-(100-x) P_2O_5 with x = 30, 35, 40, 45, and 50 mol% glasses were prepared from stoichiometric powders resulting from the mixing of hydrogen ammonium phosphate ($NH_4H_2PO_4$) and strontium carbonate ($SrCO_3$). These precursors were weighed in a micro analytical balance and mixed thoroughly according to appropriate molar compositions. The mixture was first heated at 350°C for 24 hours in an alumina crucible placed in an electric furnace in order to evaporate ammonia and water. Then, the temperature of the furnace is increased to reach the melt for about 2 hours at 1100°C. The molten samples were quenched

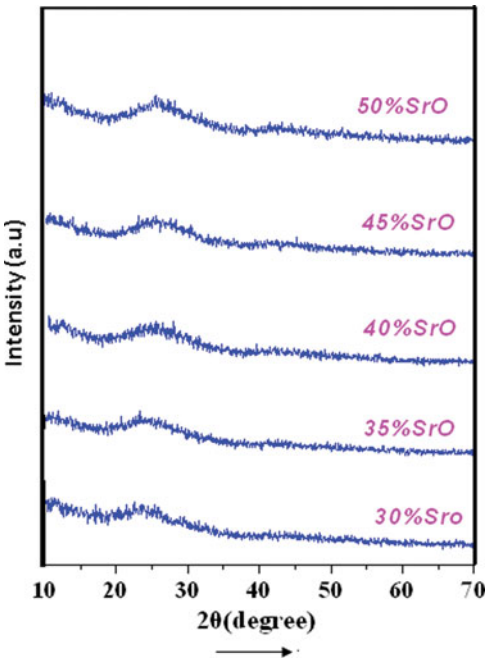

Figure 1. XRD patterns of xSrO-(100-x) P_2O_5, glass powders at room temperature.

by pouring on a stainless steel. The glass samples were kept in desiccators to prevent possible attack by moisture until used.

The amorphous nature of the as-quenched samples was verified using the X-ray diffraction technique. The glass density was carried out at room temperatures using the Archimedes method with diethyl orthophtalate as the immersion fluid (d = 1.118 g/cm3 at 25°C). The relative error in these measurements was about ±0.01 g/cm3. The density is calculated using the formula [14]:

$$d = d\text{orth}\frac{Wair}{Worth}$$

Where, W_{air} is the weight of the glass sample in air, W_{ortho} is the weight of the glass sample in orthophtalate and d_{orth} is the density of orthophtalate. The molar volume of the glass samples can be calculated from following expression:

$$Vm = \sum \frac{XiMi}{d}$$

Where, V_m is the molar volume, d is the density, Xi represent the molar fraction and Mi is the molecular weight of the ith component.

Infrared absorption measurements were made on KBr pellets (3 wt.%) in the frequency range 400–1500 cm^{-1} at room temperature using a device like FTIR- 8400S(C E) SHIMADZU. All measurements were at 4 cm^{-1} resolution. Raman spectra of glasses were recorded by a Raman spectrometer (TF FRA 106/S model) on powder samples at room temperature in the range 200–1400 cm^{-1}.

Table 1. Glass compositions (mol %), molecular weight M (g/mol), density d (g/cm3), and molar volume V_m (cm^3/mol) of xSrO-(100-x) P_2O_5 glasses.

%mol SrO	% mol P_2O_5	Average molecular weight M (g/mol)	Density d (±0 .01 g/cm^3)	Molar volume Vm (cm^3/mol) (±0 .01)
30	70	130.486	1 .98	65.90
35	65	128.567	2.32	55.416
40	60	126.648	3.22	39.331
45	55	124.729	3, 58	34.840
50	50	122.810	4.01	30.625

3. Results and discussion

X-ray diffraction (XRD) analysis

The XRD patterns of the xSrO-(100-x) P_2O_5 (x = 30, 35, 40, 45, and 50%) glass samples are shown in Figure 1. They show no continuous and discrete sharp peak, but exhibit broad halo which reflects the characteristics of amorphous glass structure.

The absence of long-range atomic arrangement is a clear indication of glassy nature of the glass samples [15, 16].

Physical properties

The change in atomic geometrical configuration, co-ordination number, cross-link density and the dimensions of the interstitial space in the glass network decides the density. Hence, the density is a tool in revealing the degree of change in the structure with the glass composition.

Table 1 display the calculated values of density (d) and molar volume (V_m) for the strontium phosphate and investigated glass samples. In the other hand, variation of density (d) and molar volume (V_m) with SrO content (mole%) for glass samples is shown in Figure 2.

From these two figures, it is clear that, the value of density increased from 1.98 to 4.01 g/cm^3 while the values of the molar volume, decreased from 65.90 to 30.625 cm^3 with the gradual increase of the SrO content in the strontium phosphate glasses. This decrease in the molar volume can be attributed to the larger packing factor of SrO. In fact, the addition of Sr^{2+} atoms changes the glass structure by creating non–bridging oxygen (NBOs) in the network. The

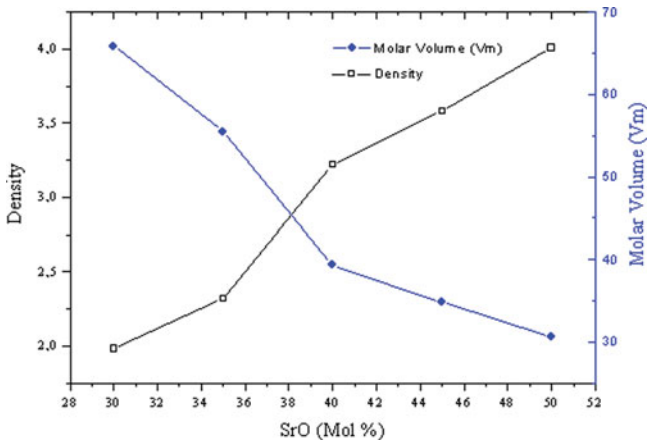

Figure 2. Variation of density and molar volume of glass with strontium oxide concentration.

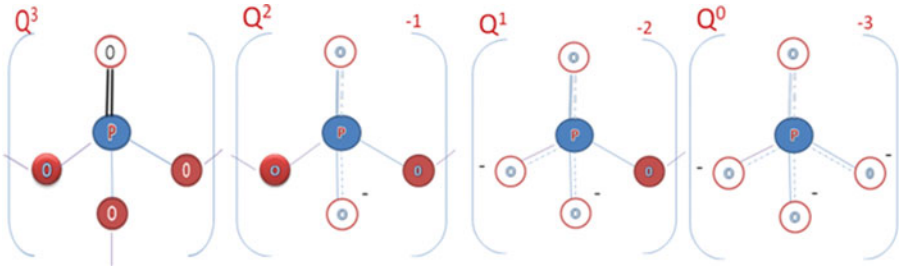

Figure 3. Q^s groups model of phosphate glasses.

NBOs created were believed to alter the glass structure in a way that the packing of molecule becomes denser as more network modifier ions (in this case Sr^{2+}), attempt to occupy the interstices with in the network. The results from this work are consistent with several studies by others on the phosphate-based glasses, for example the density of tin boro-phosphate glasses increases with B_2O_3 compositions and the molar volume V_m gradually decreases with increasing B_2O_3 concentration [17]. A similar trend was found in lead-bismuth phosphate glasses, the values of the density of the glasses increase accompanying the addition of Bi_2O_3, is probably due to a change in cross-link density and coordination number of Bi^{3+} ions [18].

FT-IR spectra analysis

The network of phosphate glasses contains a polymeric structure dominated by linkages between PO_4 tetrahedra. In the case of vitreous P_2O_5, these groups are connected to adjacent units by three of their four vertices; one place is occupied by a terminal, double-bonded oxygen atom (DBO).

Many authors [19–21] have proposed the formation of different phosphate structural groups (units) during the reorganization processes accompanying the addition of some modifier oxides (Na_2O, Li_2O, CaO etc.). They assumed that the doubly bonded oxygens are related to the number of alkali added and the number of non-bridging oxygens (NBOs) created.

The structures of binary phosphate glasses are described by so-called Qs group's model. The phosphate structural groups (Figure 3) pass from Q^3 to Q^2 to Q^1 to Q^0 as the ratio $M_2O/P_2O_5 = R$ passes from 0 to 1, 2 and finally to 3 [19, 22].

IR spectra in the frequency range 400 cm^{-1}-1500 cm^{-1} of the glasses xSrO-(100-x)P_2O_5 system at room temperature are characteristic of phosphate glasses. Figure 4 shows the obtained IR spectra for these glasses. It c an be observed several absorption bands localized around 1384, 1100, 1040, 930, 770, 720, 520 and 484 cm^{-1}.

The attribution of the absorption bands is done by comparison of our results with data given in the literature.

The fundamental and strong broad absorption band at 1384cm^{-1} is attributed to the asymmetric stretching vibration of P = O bond [23, 24].

The strong band at 1100 cm^{-1} is attributed to asymmetric stretching modes, $\nu_{as}(PO3)^{2-}$, of pyrophosphate groups. The weak band at 1040 cm^{-1} is assigned to symmetric stretching mode of $(PO_3)^{2-}$ units [25]. The band at 930 cm^{-1} is attributed to the asymmetric vibrations ν_{as}(P–O–P) of bridging oxygen atoms in phosphate chains [26].

The band at 720 and 770 cm^{-1} may be attributed to symmetric stretching vibrations, ν_s(P–O–P), of bridging oxygen atoms [25–27].

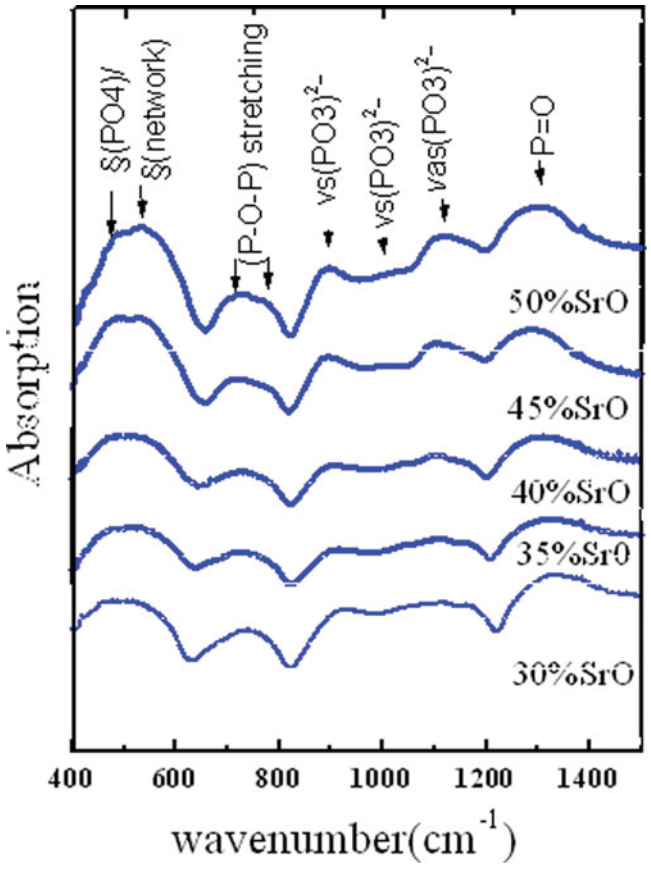

Figure 4. IR absorption spectra of glasses xSrO - (100-x) P_2O_5 system.

The broad band around 520 cm^{-1} and 475 cm^{-1} belongs to the bending vibrations of basic structural units of phosphate glasses [28–30].

The summary of the data on the positions of various bands of IR spectra assignments is presented in Table 2.

The intensity of ν_{as} (P = O) gradually decreases with increasing SrO content, this band may also consist of bands due to asymmetrical vibrations of $(PO_2)^-$ mode, ν_{as} $(PO_2)^-$, in metaphosphate units of ten called Q^2 units. The Q^2 units has two NBOs, which are usually assumed to be different since the first terminal oxygen is bonded by P = O while the other terminal oxygen forms P-O- bond. An increase in the P-O-P asymmetric bending vibrations evidenced from IR spectra, which shifts from 925 to 943 cm^{-1}, is a characteristic of transition from chains to pyrophosphates which enhance the disorderliness in the glass network [31],

Table 2. Various bands in the IR spectra of SrO-P_20_5 glasses.

Structural group	P = O stretching (cm^{-1})	$\nu_{as}(PO3)^{2-}$(cm^{-1})	$\nu s(PO3)^{2-}$ (cm^{-1})	ν_{as}(P–O–P)	(P–O–P) stretching		δ(PO4)/δ(network)	
30%SrO-70%P_20_5	1384	1111	1037	929	727	776	484	513
35%SrO-65%P_20_5	1384	1111	1040	925	727	764	489	520
40%SrO-60%P_20_5	1383	1114	1040	928	725	770	484	518
45%SrO-45%P_20_5	1383	1107	1039	929	719	767	489	520
50%SrO-50%P_20_5	1383	1111	1045	943	723	764	484	500

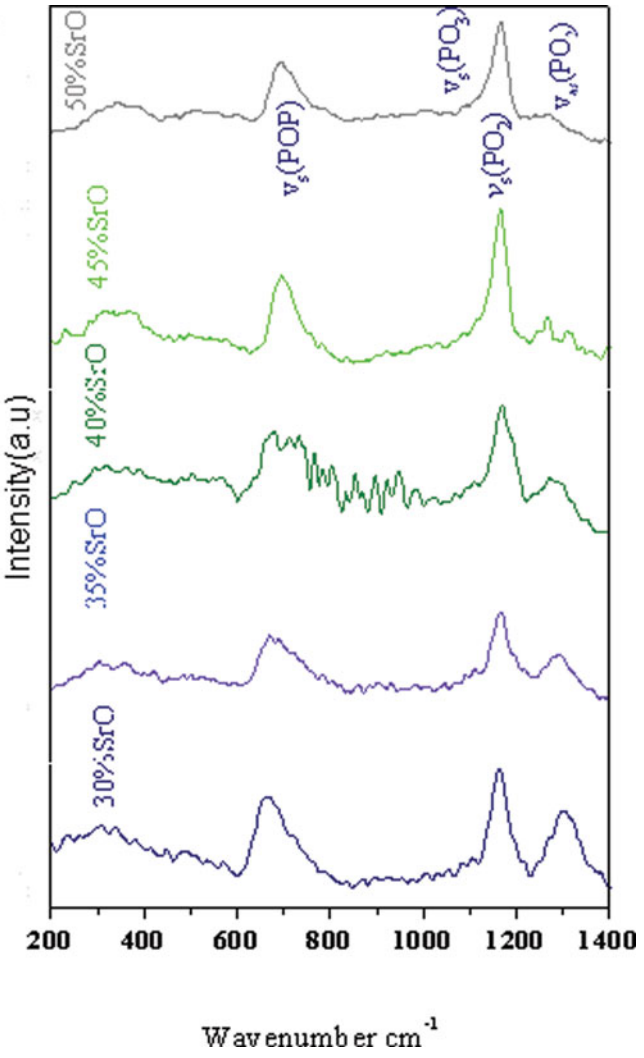

Figure 5. Raman spectra of the glasses xSrO - (100-x) P_2O_5 System.

also the shifting of ν_{as}(P–O–P) bands towards higher wavenumbers when SrO increases, a similar trend is noted for the IR spectra for glasses of SrO-TiO_2-P_2O_5 when the amount P_2O_5 (or TiO_2) decreases (or increases) [32]. The variation of the frequency of P-O-P bonds, with increasing SrO content, is due to the breakage of cyclic P-O-P bonds in the glass when the strontium oxide act as network modifier and both bands are shifted towards lower frequency. The addition of the modifier oxide SrO at P_2O_5 lead to the creation of non-bridging oxygen atoms at the expense of the bridging oxygen atoms,

Raman spectra

Raman spectra of the glasses xSrO-(100-x) P_2O_5 were plotted in Figure 5. As the increase of SrO in each glass series leads to significantly changes in Raman spectra. The assignments of different observed bands are listed as follows:

(i) The band at about 1296 cm^{-1} is attributed to PO_2 asymmetrical stretching modes, $\nu_{as}(PO_2)^-$, related to Q^2 tetrahedra [33]. It decreases in relative amplitude and moves to smaller wavenumber at 1267 cm^{-1}.

(ii) The most intense band at 1162 cm^{-1} is assigned to PO_2 symmetrical stretching modes, $\nu_s(PO_2)^-$, associated to the O-P-O non bridging oxygens indicating the formation of Q^2 phosphate tetrahedra [34,35]. This band increases significantly in relative amplitude and shifts to lower wavenumber (1162–1170 cm^{-1})

(iii) The weak band at 1100 cm^{-1} is attributed to symmetric vibration of the non-bridging oxygen (PO_3) in Q^1 tetrahedra, $\nu_s(PO_3)^{2-}$ [36, 37].

(iv) The band at 662 cm^{-1} decreases in relative amplitude and shifts to a greater wavenumber (662–693 cm^{-1}), this band is assigned to symmetrical stretching vibration (POP)sym of bridging oxygen atoms between Q^3tetrahedra, [36,37].

(v) Two weak bands at low wavenumber (358 and 533 cm^{-1}) shift slightly at the higher frequency and their relative amplitudes decrease slightly with increasing SrO. These two bands have usually been attributed to bending modes related to cation motion and phosphate tetrahedra [38,39].

The relative intensity of the $\nu_{as}(PO_2)^-$ band at ∼1267–1296 cm^{-1}, decrease with increasing SrO content [40]. The assignment of the band centered at ∼1267 cm^{-1} represente a problem. Based on several studies of ν-P_2O_5 found in literature, Hudgens et al. [35] studied the structure of lithium ultraphosphate glasses. It was observed that the band assigned to P = O terminal oxygens, centered at ∼1390 cm^{-1}, decreases in wavenumber to∼1260 $cm^{-}1$ with the increasing of the alkali oxide from 20 to 50 mol%. Weeks and Bray [41]., observed that the band assigned to P = O terminal oxygens, centered at ∼1390 cm^{-1}, shifts to ∼1250 cm−1 with the increasing of the metal oxide from 20 to 50 mol% and became indistinguishable from the $\nu_{as}(PO_2)$ mode of a Q^2 tetrahedron. Its wavenumber is ascribed to an increase in average length of the P = O bond resulting from π-bond delocalization on the Q^3 tetrahedra. The explanation was that this decreasing in wavenumber is due to an increase in average length of the P = O bond resulting from π-bond delocalization on the Q^3 tetrahedra.

The band at 1170 cm^{-1}, which is believed to be related with the symmetrical stretching vibrations vs(PO2) of two non-bridging oxygens in the[PO4]. And it shifts to lower frequencies with the substitution of SrO for P_2O_5, indicates the decreases in O–P–O band angle, a similar trend was observed in the infrared spectra from $2Al_2O_3$-xSrO–(18-x)ZnO-33.3P_2O_5–16.7B_2O_3– 30SiO_2 glasses as a function of SrO and ZnO content [11].

The addition of SrO results in gradual depolymerization of the phosphate chains and formation of short phosphate units will remain by and large as terminal groups. However, SrO is a well-known modifier and may enter into glass network by transforming two Q^3 tetrahedra into two Q^2 tetrahedra and thus, the formed SrO polyhedron is surrounded by two Q^2 and several Q3 tetrahedra. This structure behaves like the structural defect in the network of P_2O_5.

4. Conclusions

The present study analyzed the physical and structural properties of P_2O_5-SrO glasses. The amorphous state of samples was verified by X-ray diffraction (XRD). The density and the molar volume were dependent on the SrO content in the glass compositions. The IR and Raman spectra suggest that the sample glasses structure has similar structures consisting of randomly distribution of Q^3, Q^2 and Q^1 structural units. The presents of Q^1(pyrophosphate) in the ultraphosphate due to disproportionatly of the type $2Q^2 \leftrightarrow Q^1 + Q^3$ which occur in these glass. All the symmetric and asymmetric stretching vibrations of POP and PO_2 observed in the spectra are characteristic of Q^3 and Q^2 groups.

References

[1] Hudgens, J. J., Brow, R. K., Tallant, D. R., & Martin, S. W. (1998). *J. Non-Cryst. Solids*, *21*, 223.
[2] Pillai, C. G. S., Sudarsan, V., Roy, M., & Dua, A. K. (2003). *J. Non-Cryst. Solids*, *313*, 321.
[3] Brow, R. K. (2000). *J. Non-Cryst. Solids*, *1*, 263–264.
[4] Chahine, A., Et-tabirou, M., & Pascal, J. L. (2004). *Mater. Lett*., *58*, 2776.
[5] Moguš-Milanković, A., Šantić, A., Gajović, A., & Day, D. E. (2003). *J. Non-Cryst. Solids*, *76*, 325.
[6] Reis, S. T., Faria, D. L. A., Martinelli, J. R., Pontuschka, W. M., Day, D. E., & Partiti, C. S. M. (2002). *J. Non-Cryst. Solids*, *188*, 304.
[7] Oh, S., Kang, M., & Chung, S. (1997). *J. Korean Physical Society*, *31*, 664–670.
[8] Egorysheva, A. V., Volodin, V. D., Milenov, T., Rafailov, P., Skorikov, V. M., & Dudkina, T. D. (2010). *Russian Journal of Inorganic Chemistry*, *55*, 1810–1817.
[9] Shih, P. Y., & Shiu, H. M. (2007). *Mater. Chem. Phys*., *106*, 222.
[10] Weng, C. Z., Chen, J. H., & Shih, P. Y. (2009). *Mater. Chem. Phys*., *115*, 628.
[11] Luo, Zhi-wei, Lu, An-xian, Chen, Bo, Zhou, Jun-lin, & Ren, Fang (2011). *Physica B*, *406*, 4558–4563.
[12] Chu, C. M., Wu, J. J., Yung, S. W., Chin c, T. S., Zhang, T., & Wu, F. B. (2011). *Journal of Non-Crystalline Solids*, *357*, 939–945.
[13] Massera, J., Kokkari, A., Närhi, T., & Hupa, L. (2015). *J. Mater. Sci. Mater. Med*., *26*, 196.
[14] Sidek, H. A. A., Hamezan, M., Zaidan, A. W., Talib, Z. A., & Kaida, K. (2005). *Am. J. Appl. Sci*., *2*, 1266.
[15] Sardar, D. K., Gruber, J. B., Zandi, B., Hutchinson, J. A., & TrusselL, C. W. (2003). *J. Appl. Phys*., *93*, 2041.
[16] Franks, K., Salih, V., Knowles, J. C., & Olsen, I. (2002). *J. Mater. Sci.: Mater. Med*., *13*, 549.
[17] Lim, J. W., Schmitt, M. L., Brow, R. K., & Yung, S. W. (2010). *J. Non-Cryst. Solids*., *356*, 1379.
[18] Saddek, Y. B. (2004). *Mater. Chem. Phys*., *83*, 222.
[19] Moustofa, Y. M., & El-Egili, K. (1998). *J. Non-Cryst. Solids*, *240*, 144.
[20] Magdas, D. A., Cozar, O., Ardelean, I., & David, L. (2007). *J. Optoelectron. Adv. Mater*., *9*, 730.
[21] Vedeanu, N., Cozar, O., & Ardelean, I. (2007). *J. Optoelectron. Adv. Mater*., *9*, 698.
[22] Lippma, E., Magi, M., Samoson, A., Englehardt, G., & Grimmer, A. R. (1980). *J. Am. Chem. Soc*., *102*, 4889.
[23] Higazy, A. A., & Bridge, B. (1985). *J. Mater. Sci*., *20*, 2345.
[24] Hudgens, J. J., & Martin, S. W. (1994). *J. Am. Ceram. Soc*., *76*, 1691.
[25] Ouchetto, M., Elouadi, B., & Parke, S. (1991). *Physics and Chemistry of Glasses*, *32*, 22.
[26] Aomari, K., Saidi, M., & Drissi, I. (1997). *Phys. Chem Glasses*, *38*, 15.
[27] Kamitsos, E. I., Kapoutsis, G. A., Chryssikos, G. D., Hutchinson, J. M., Pappin, A. J., Ingram, M. D., & Duffy, J. A. (1995). *Phys. Chem. Glasses*., *36*, 141.
[28] Mouhsine, N., Allali, N., Bih, L., Yacoubi, A., & Nadiri, A. (2004). *Physical and Chemical News*, *19*, 130.
[29] Ahmed, J., Lewis, M., Olsen, J., & Knowles, J. C. (2004). *Biomaterials*, *25*, 491.
[30] Doweidar, H., Moustafa, Y. M., El-Egili, K., & Abbas, I. (2005). *Vibr. Spectrosc*., *37*, 91.
[31] Rulmont, A., Cahay, R., & Tarte, P. (1991). *Eur. J. Solid State Inorg Chem*., *28*, 207.
[32] Sinouh, H., Bih, L., & Azrour, M. (2012). *Journal of Physics and Chemistry of Solids*, *73*, 961–968.
[33] Garrigou-Lagrange, C., Oucheto, M., & Elouadi, B. (1985). *Can. J. Chem*., *63*, 1436.
[34] Ardelean, I., Rusu, D., Andronache, C., & Ciobotă, V. (2007). *Mater. Leters*, *61*, 3301.
[35] Hudgens, J. J., Brow, R. K., Tallant, D. R., & Martin, S. W. (1998). *J. Non-Cryst. Solids*, *223*, 21.
[36] Brow, R. K., Tallant, D. R., Myers, S. T., & Phifer, C. C. (1995). *J. Non-Cryst. Solids*, *191*, 45–55.
[37] Zhang, L. Y., & Brow, R. K. (2011). *J. Am. Ceram. Soc*., *94*, 3123.
[38] Šantić, A., Moguš-Milanković, A., Furić, K., Bermanec, V., Kim, C. W., & Day, D. E. (2007). *J. Non-Cryst. Solids*, *353*, 1070.
[39] Moguš-Milanković, A., Šantić, A., Ličina, V., & Day, D. E. (2005). *J. Non-Cryst. Solids*, *351*, 3235.
[40] Hussin, R., Aziz, N. A. S., Rohaizat, A., Deraman, K., Nurulhuda, W., Shamsuri, W., Fazliana Abdul Halim, D. N., Husin, M. S., Ahmad, N. E., Hashim, I. H., & Ismail, B. (2011). *Solid State Science and Technology*, *19*, 363.
[41] Ivascu, C., Cozar, I. B., Daraban, L., & Damian, G. (2013). *Journal of Non-Crystalline Solids*, *359*, 60–64.